Electronic Supplementary Material (ESI) for Soft Matter.

Supplementary Information

How Hydrogen-bonding Interactions and Nanocrystal Aspect Ratio Influence the Morphology and Mechanical Performance of Polymer Nanocomposites Reinforced with Cellulose Nanocrystals

*Chuanwei Miao[a], Damien Maura[c], and Wadood Y. Hamad,[a,b,]**

[a] Transformation and Interfaces Group, Bioproducts Innovation Centre of Excellence, FPInnovations, 2665 East Mall, Vancouver, British Columbia, Canada V6T 1Z4

[b] Department of Chemistry, University of British Columbia, 2306 Main Mall, Vancouver, BC, Canada V6T 1Z1

[c] Bioproducts Innovation Centre of Excellence, FPInnovations, 570 Saint-Jean Blvd, Pointe-Claire, QC Canada H9R 3J9

*Corresponding author: wadood.hamad@fpinnovations.ca, Tel. +1+604 225 5839

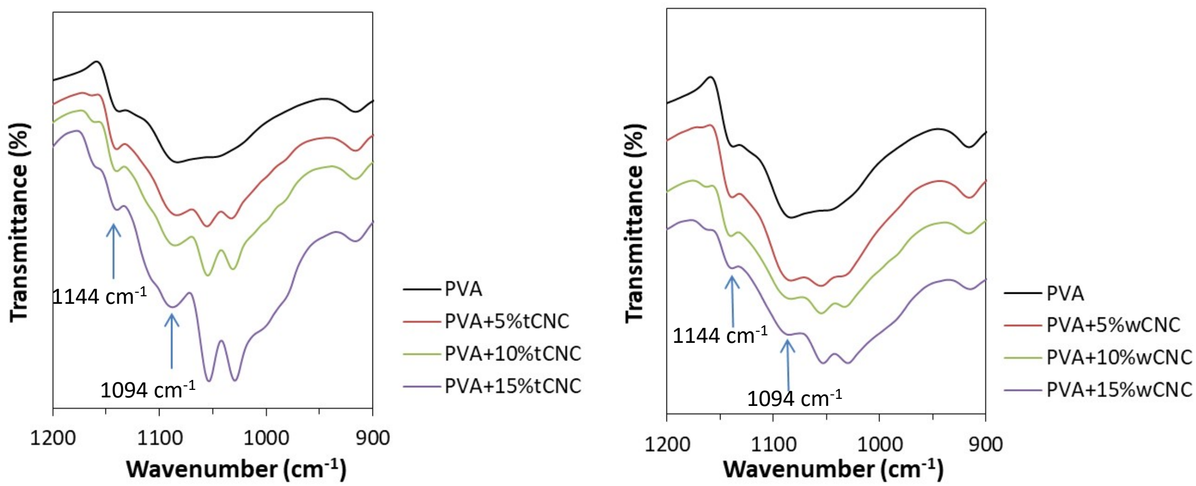

Fig. S1. FTIR spectra for calculating the crystallinity degree of PVA.

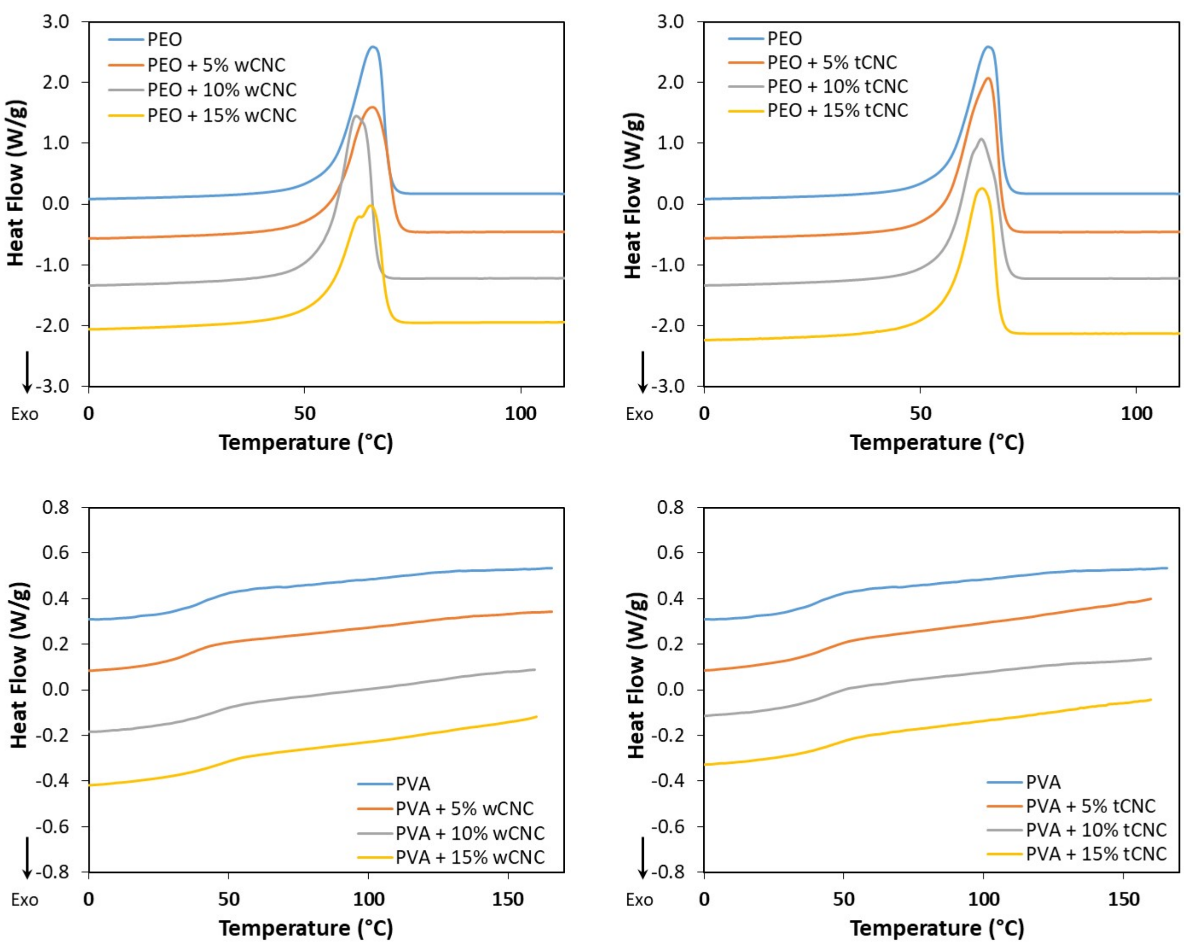

Fig. S2. DSC curves of PEO, PVA, and their nanocomposites reinforced with wCNC or tCNC.

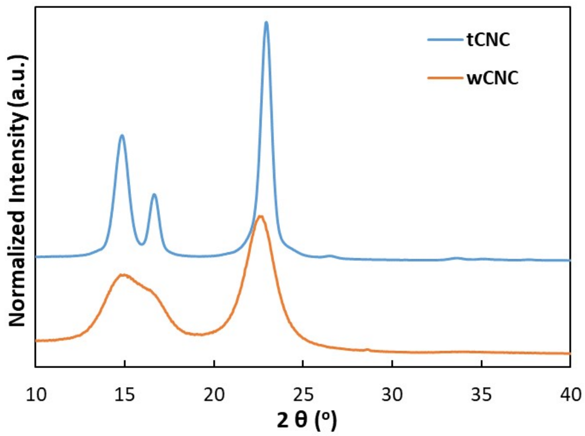

Fig. 3. X-ray diffraction patterns of wCNC and tCNC illustrating the crystal structures of wCNC and tCNC are cellulose I_β and cellulose I_α, respectively, which is ascribed to their different sources.

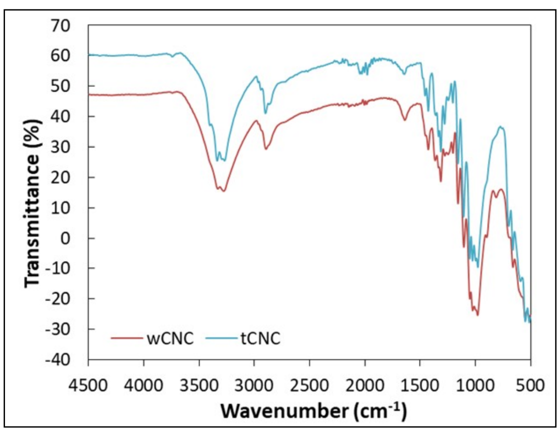

Fig. S4. Full FTIR spectra of wCNC and tCNC.

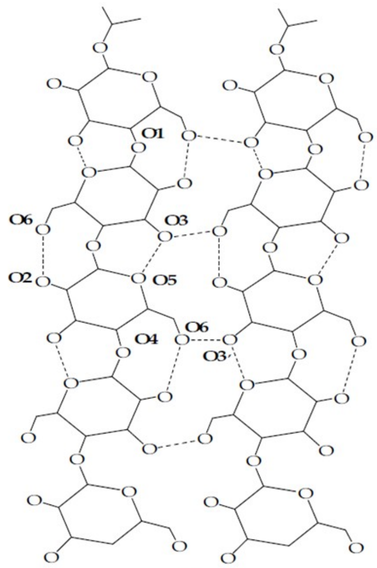

Fig. S5. Formation of intra-molecular hydrogen bonding, O(2)H-O(6) and O(3)H-O(5), and inter-molecular hydrogen bonding, O(6)H-O(3'), between parallel cellulose chains (Fan, Dai, & Huang, 2012).

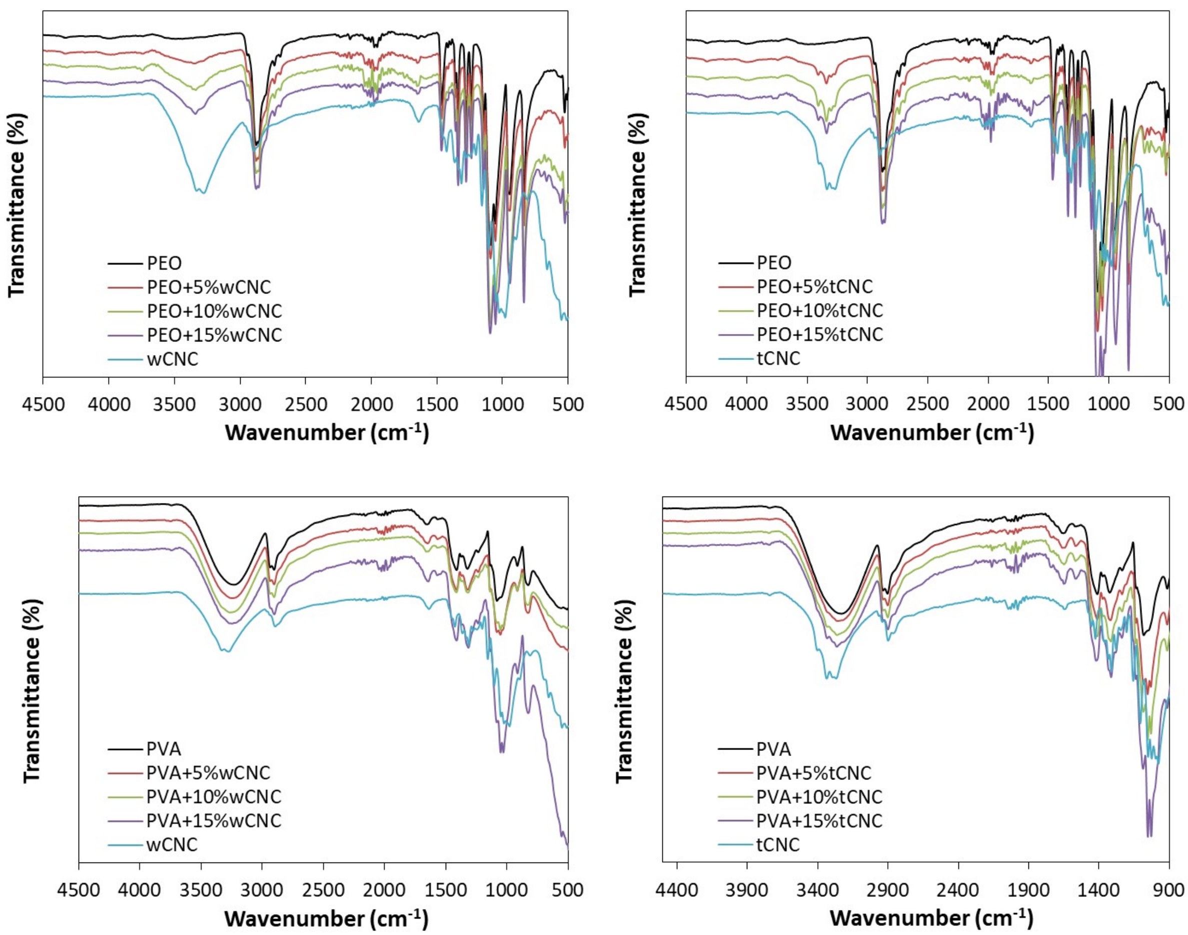

Fig. S6. Full FTIR spectra of PEO, PVA, and their nanocomposites with wCNCs or tCNCs.

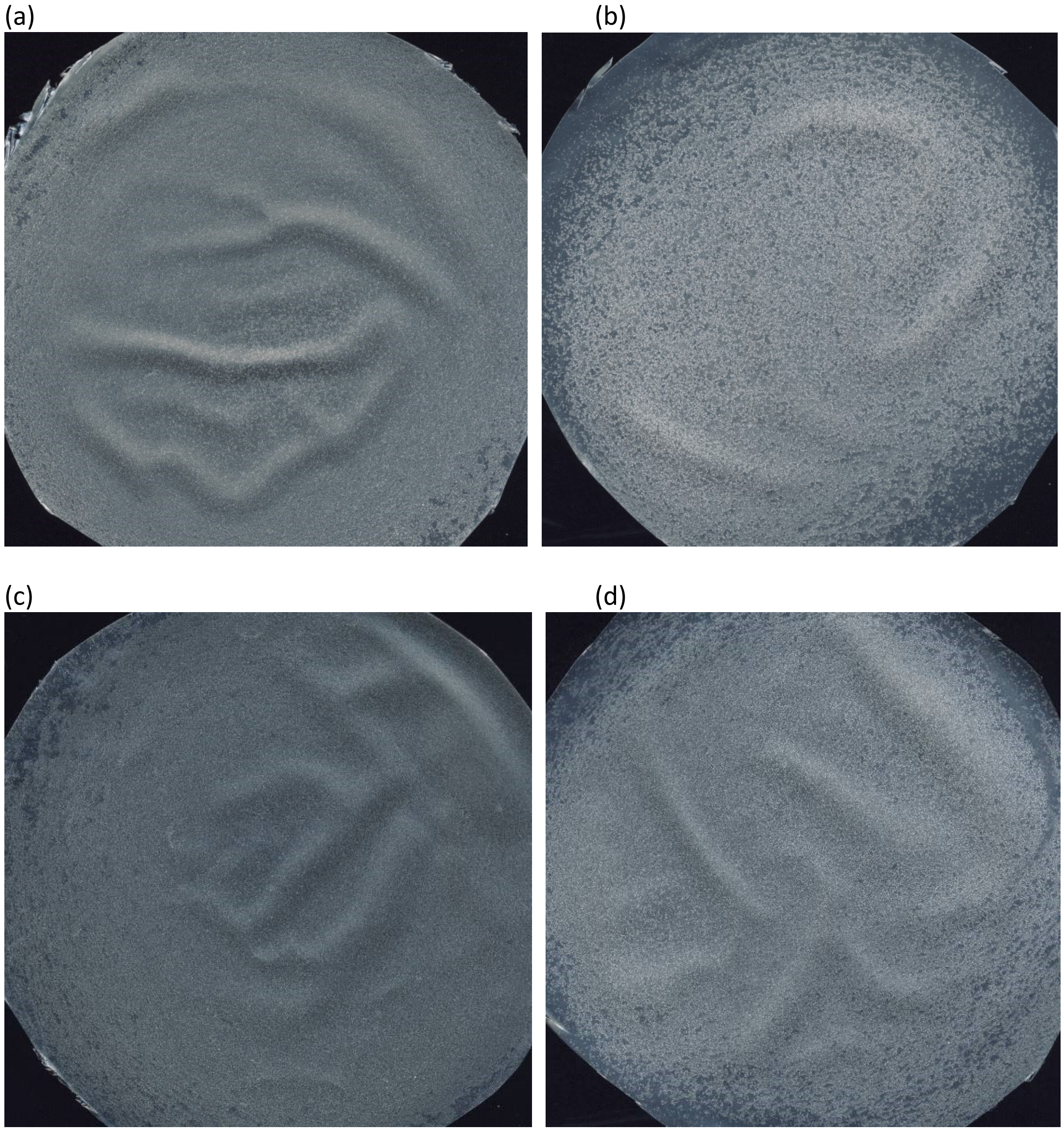

Fig. S7. Photos of cast films of (a) PEO-5-wCNC, (b) PEO-5-tCNC, (c)PEO-10-wCNC, and (d) PEO-10-tCNC. The diameter of films is 15 cm.

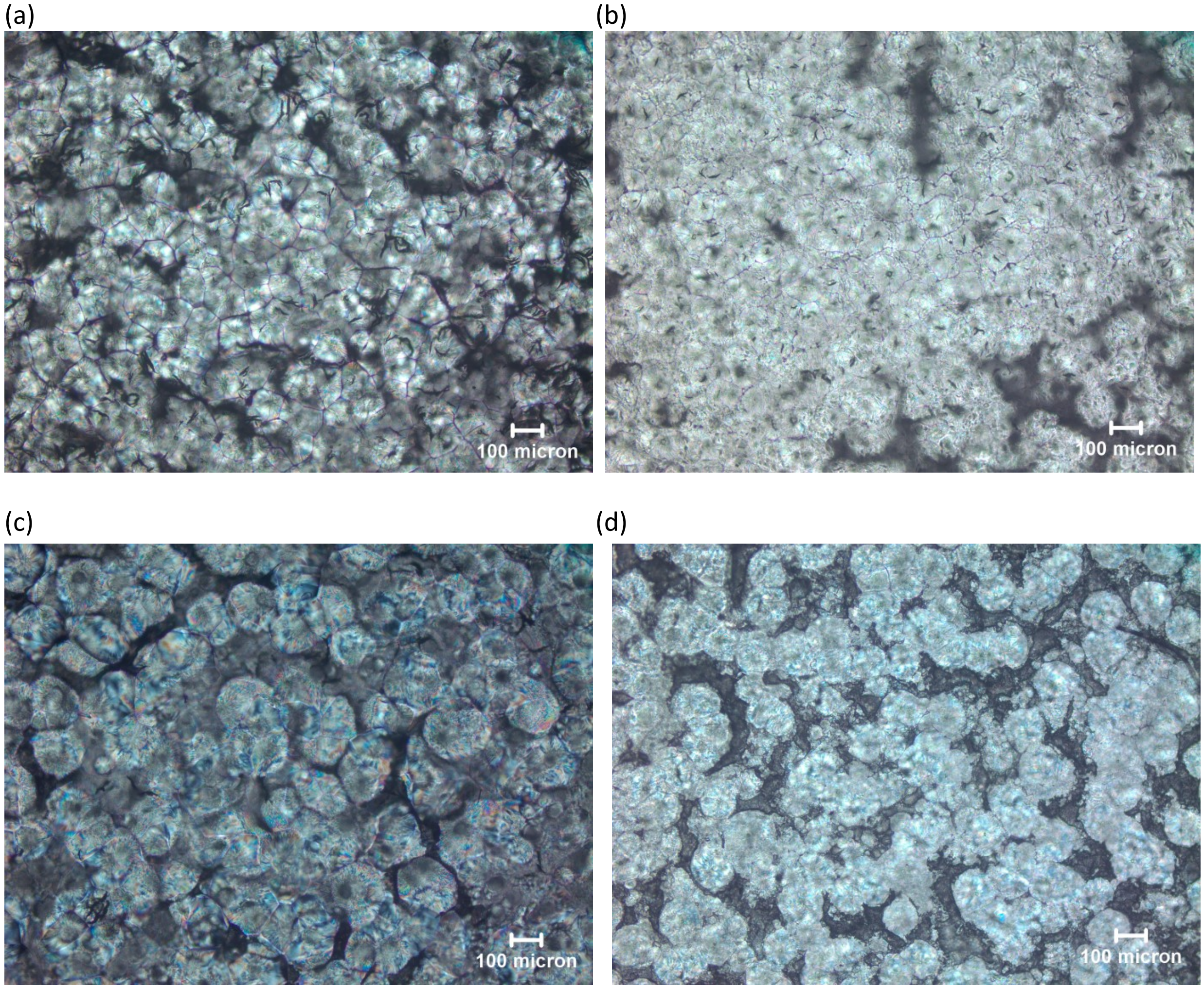

Fig. S8. POM images of (a) PEO-5-wCNC, (b) PEO-5-tCNC, (c) PEO-10-wCNC, and (d) PEO-10-tCNC cast nanocomposite films.

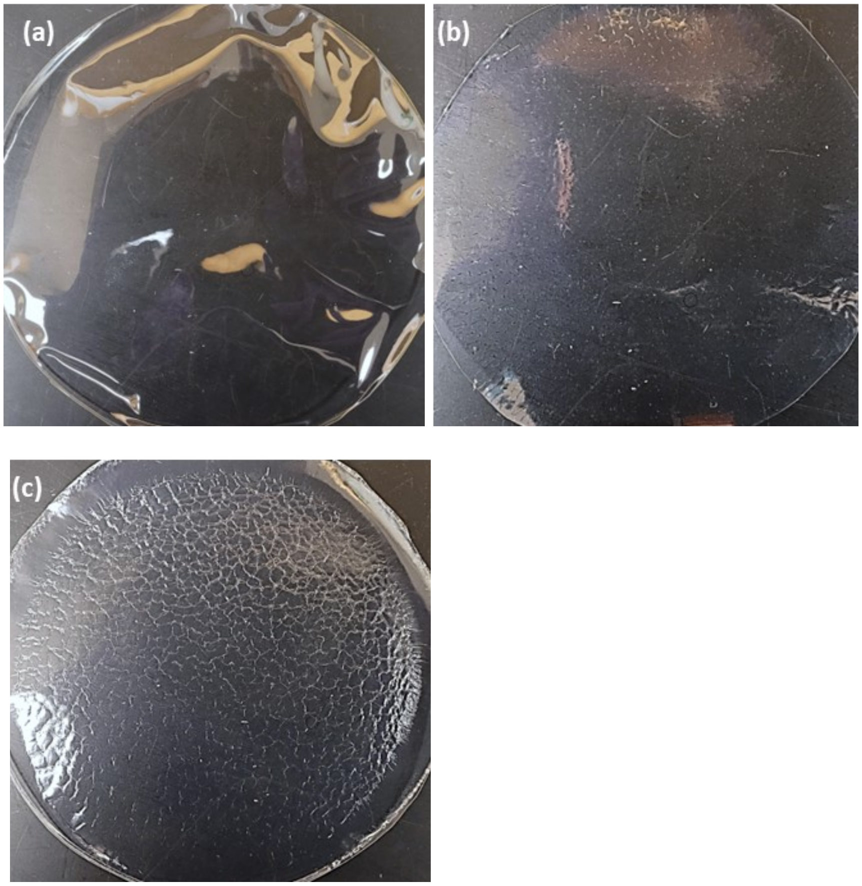

Fig. S9. Photos of (a) neat PVA, (b) PVA-10-wCNC, and (c) PVA-10-tCNC films.

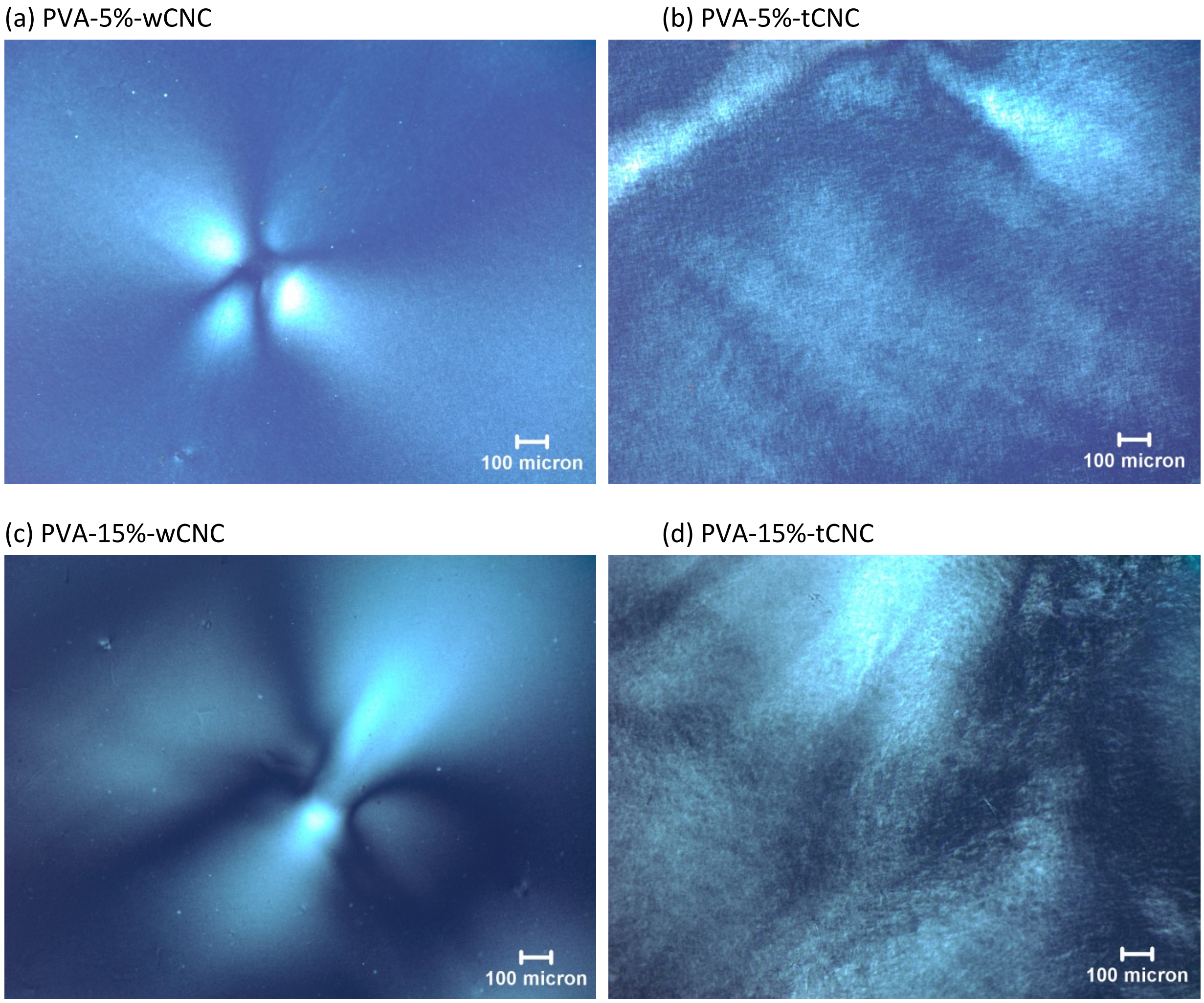

Fig. S10. POM images of PVA and its nanocomposite films.

Table S1. Elemental analysis summary for wCNCs and tCNCs.

	C (%)	H (%)	O (%)	N (%)	S (%)
wCNCs	39.22	5.98	48.69	<0.30	0.73
tCNCs	42.60	5.90	47.71	<0.30	<0.30

Table S2. Degrees of crystallinity for neat polymers and nanocomposite films at different CNC contents based on calculations using DSC (for PEO) and FTIR (for PVA) data.

	Neat	**[wCNC]**			**[tCNC]**		
	Polymer	**5%**	**10%**	**15%**	**5%**	**10%**	**15%**
PEO	69 %	71 %	73 %	65 %	72 %	72 %	70 %
PVA	43 %	43 %	45 %	40 %	42 %	42 %	41 %

Table S3. Summary of the tensile properties of PEO and PEO/CNC nanocomposites and their levels of change relative to neat PEO.

Nanocomposite and CNC content (wt. %)		**Young's Modulus (MPa)**			**Strength at Yield (MPa)**			**Strain at Break (%)**		
		Ave.	**Sdv.**	**Change**	**Ave.**	**Sdv.**	**Change**	**Ave.**	**Sdv.**	**Change**
Neat PEO		617	82	-	10.5	1.4	-	32	1.9	-
PEO-wCNC	**5%**	840	33	36%	15.3	0.9	46%	684	96	2038%
	10%	1309	77	112%	20.0	0.7	91%	691	63	2059%
	15%	1220	85	98%	19.1	0.9	82%	646	64	1919%
PEO-tCNC	**5%**	1185	25	92%	18.6	0.6	77%	75	37	134%
	10%	1553	63	152%	23.6	1.0	125%	28	15	-13%
	15%	1857	55	201%	29.2	0.6	178%	38	14	19%

Table S4. Summary of the tensile properties of PVA and PVA/CNC nanocomposites and their levels of change relative to neat PVA.

Nanocomposite and CNC content (wt. %)		Young's Modulus (MPa)			Strength at Yield (MPa)			Strain at Break (%)		
		Ave.	Sdv.	Change	Ave.	Sdv.	Change	Ave.	Sdv.	Change
Neat PVA		2457	291	-	54.2	6.1	-	210	85	-
PVA-wCNC	5%	2723	168	11%	54.5	3.2	1%	228	75	9%
	10%	3461	120	41%	65.7	1.3	21%	224	90	7%
	15%	3842	137	56 %	69.0	3.2	27%	188	98	-11%
PVA-tCNC	5%	3248	214	32%	87.1	2.7	61%	85	35	-60%
	10%	3256	221	33%	90.6	3.4	67%	8	2	-96%
	15%	2686	103	9%	88.1	2.9	63%	6	1	-97%

Table S5. The glass transition temperature (T_g) and peak melting temperature (T_m) of PEO/CNC and PVA/CNC nanocomposites determined by DSC.

	T_g (°C)				T_m (°C)			
[CNC] %	**0**	**5**	**10**	**15**	**0**	**5**	**10**	**15**
PEO-wCNC	-	-	-	-	65.5	65.5	61.3	62.0 & 65.0
PEO-tCNC	-	-	-	-	65.5	65.5	64.0	64.4
PVA-wCNC	44.3	43.1	43.3	46.1	-	-	-	-
PVA-tCNC	44.3	43.3	43.3	45.2	-	-	-	-

Reference

Fan, M., Dai, D., & Huang, B. (2012). *Fourier transform infrared spectroscopy for natural fibres*. In S. Salih (Ed.), *Fourier transform-materials analysis* (pp. 45-68): InTech